This is the peer reviewed author accepted manuscript (post print) version of a published work that appeared in final form in:

Alder, Fiona A, Charrault, Eric, Zuber, Kamil, Fabretto, Manrico, Patil, Apurva, Murphy, Peter & Llusca, Marta 2020 'Fabrication of robust solar mirrors on polymeric substrates by physical vapor deposition technique', *Solar Energy Materials and Solar Cells* vol. 209, article no. 110476, pp. 1-7

This output may not exactly replicate the final published authoritative version for which the publisher owns copyright. It is not the copy of record. This output may be used for non-commercial purposes. This version is licensed under a Creative Commons CC-BY-NC-ND 4.0 license (http://creativecommons.org/licenses/by-nc-nd/4.0/).

The final definitive published version (version of record) is available at:
https://doi.org/10.1016/j.solmat.2020.110476

Persistent link to the Research Outputs Repository:
http://researchoutputs.unisa.edu.au/11541.2/141712

General Rights
Copyright and moral rights for the publications made accessible in the Research Outputs Repository are retained by the authors and/or other copyright owners and it is a condition of accessing publications that users recognize and abide by the legal requirements associated with these rights.

- Users may download and print one copy for the purpose of private study or research.
- You may not further distribute the material or use it for any profit-making activity or commercial gain
- You may freely distribute the persistent link identifying the publication in the Research Outputs Repository

If you believe that this document breaches copyright please contact us providing details, and we will remove access to the work immediately and investigate your claim.

Fabrication of robust solar mirrors on polymeric substrates by physical vapor deposition technique

[1]Fiona. A. Alder, [2]Eric Charrault, [2]Kamil Zuber, [2]Manrico Fabretto, [2]Apurva Patil, [2]Peter Murphy, [2]Marta Llusca*

[1]*Department of Natural Sciences, University of Bath, Bath, BA2 7AY, United Kingdom*
[2]*Thin Films Coating Group, Future Industries Institute, University of South Australia, Mawson lakes, 5095 South Australia, Australia.*

*corresponding author: marta.lluscajane@unisa.edu.au

Abstract:

Aluminium, first surface, plastic mirrors have been developed to be used as heliostats in concentrated solar power stations. The Al reflective layer, the adhesion of the reflective layer to the polycarbonate (PC) substrate and the protective over-coat have all been optimised in order to achieve a highly reflective, robust and durable light-weight mirror. The Al layers were deposited by means of magnetron sputtering and the change in reflectance was investigated as a result of variations in the sputtering conditions. The influence of the substrate cleaning process and the addition of an interfacial seed layer on the adhesion of the reflective layer were also systematically studied. A thick sputtered SiO_2 film and a dip-coated transparent hard-coat resin were examined as protective coatings against weathering tests. All prepared samples were characterised using, adhesion and abrasion tests, spectrophotometry, nano-scratch, salt-spray tests and both accelerated and outdoor weathering.

The optimal three-layer stack was found to be 15 nm of SiO_2 as an adhesive layer, 80 nm of Al as the reflector and 4.5 µm dip-coated, hard-coat resin as the protective layer. The three-layer stack plastic mirror gave an overall total solar weighted specular reflectance of ≈ 88% which was maintained even after aggressive abrasion tests such as Bayer and Steel Wool, 40 days within a salt-spray chamber and after 5 months under accelerated weathering.

Keywords:

Plastic mirrors, concentrating solar power, solar mirrors, thin films, sputtering

1. Introduction

Amongst the range of renewable energy generation methods the Concentrated Solar Thermal (CST) and Concentrated Solar Photovoltaic (CSP) have been getting a rising interest. The CST power plants can generate energy both during the day and night converting stored heat into electricity. The CSP generation devices use very high efficiency triple junction solar cells typically only found in satellites due to high cost. Both of these emerging renewable energy generation methods use an array of mirrors - Heliostats focusing sunlight onto the central tower. Mirrors for solar concentrator applications must have high specular reflectance (SR), long service-life under extreme weather conditions (UV radiation, chemical pollutants, moisture) and should ideally be cost-effective to produce and install. Conventional heliostat mirrors are usually second-surface coatings, meaning that the reflective material is deposited onto the back side of the glass substrate. The disadvantage of using traditional glass substrates is their high weight and fragility, which makes handling and installation an expensive and delicate process. By way of contrast, first- or front-surface mirrors have the reflective layer located on the top surface of the substrate [1, 2], thus any substrate can be used such as metals or plastics since the requirement for optical transparency is eliminated.

Silver is typically used as the reflective metal because of its high SR of ≈ 96% in the range 280 –3300 nm [3]. However, its poor adhesion to some substrates [4, 5] and sulphide and chlorine tarnishing [6−8] make Ag-based first-surface mirrors vulnerable to degradation when exposed to environmental conditions. On the other hand, Al, although not as reflective as silver (≈ 91% in the range 280-3300 nm) [9], is cheaper and more weather resistant. Notwithstanding these two advantages, an interfacial seed layer must be used to improve Al adhesion onto the substrate, and a robust transparent protective coating (or coatings) must be positioned onto the topmost surface so as to provide environmental stability for the service-life of the mirror (i.e. 25 years or more) [10].

Different researchers have reported on the fabrication and testing of first-surface mirrors. For example, Kennedy et al. [11] developed Al mirrors deposited onto PET substrates protected with an alumina coating, and demonstrated good optical performance even after 3000 hours of accelerated weathering. Morales and Ajona [12, 13] reported on sol-gel grown SiO_2 deposited onto Al and Ag

sputtered films, which still produced good thermal stability after 240 hours at 400°C. Almanza et al. [14] produced a durable Al first surface mirror, coated with thick sputtered SiO_2, which exhibited a modest decrease of 3% in its reflectance after 12 years of natural weathering. More recently, Xu et al. [15] have reported on a sputtered Ag coating which also incorporated a SiO_2 layer as well as an alternative TiO_2/SiO_2 bilayer [16]. In a similar vein, Ennaceri et al. [17] utilised a ZnO/TiO_2 bilayer in an attempt to provide protection for Ag-based glass reflectors. The use of polymeric materials to protect Ag-based reflectors has also been researched [18-22], with the dominant task still being the negation of Ag degradation. Schissel et al. [18] improved the durability of a proprietary ECP-305 silvered-PMMA mirror (commercially available 3M product) by adding: UV absorbers to the polymer, post-annealing treatments and, protecting the substrate edges.

The aim of this work is to develop a simple, robust, low-cost and highly durable plastic mirror which will match the performance characteristics of glassed based mirrors. The use of a plastic based mirror will however not suffer from issues associated with transportation and installation, which is the hallmark of glassed based mirrors. For this purpose, polycarbonate (PC) was chosen as the substrate and sputtered Al as the reflective layer. The reflectance of the Al films was optimized by varying the thickness, the sputtering power and the pressure before and during deposition. The adhesion between Al and the PC surface was evaluated by comparing different PC substrate treatments, namely: cleaning with isopropanol, with an Ar plasma, or by adding a SiO_2 seed layer. Moreover, to protect the mirrors a sputtered SiO_2 overcoat layer and a dip-coated siloxane resin were compared. The SR, morphology, adhesion, abrasion and hardness measurements, salt-spray, accelerated environment ageing tests and natural weathering were investigated. In this work we demonstrate that the simple 3 layer stack plastic mirror consisting of a: SiO_2 seed layer, Al reflective layer and a protective overcoat layer, is able to maintain its solar weighted specular reflectance ($\overline{SR}$) of ≈ 88% after 5 months of both natural weathering and accelerated weathering. Additionally, the inherent robustness of such 3 layers architecture protects the final product from 40 day under salt-humid atmosphere and from very aggressive Bayer and Steel Wool abrasion tests.

2. Experimental details

2.1 Sample preparation

Al thin films were magnetron sputtered from a 3 inch Al target, 99.99% pure, onto commercially available hard coated polycarbonate (PC, Bayer Makrolon® AR, 7×7 cm and 4.5 mm thick), later in text referred as 'PC'. The sputtering system was an in-house built reactor and is described elsewhere [23]. Depositions were carried out at room temperature while the substrates were rotating at 60 rpm at a distance of 120 mm from the target. The Al thickness, base pressure, working pressure and the power during deposition were varied in order to maximise the reflectivity of the film.

To study the adhesion between the Al films and the substrate surface three different samples were prepared. Al was deposited onto PC cleaned by means of an Ar plasma (3 min. duration), the same Al film was grown onto isopropanol cleaned PC and, also on top of 15 nm of SiO_2 previously deposited on the substrate. The SiO_2 thin film was sputtered at 1100 W in the poison mode (i.e. maintaining a deposition process while the surface of the target is oxidized, with the process voltage/current characteristics far different than in the "metallic mode" [24]) from a Si target (99% pure), 150×320 cm, under and oxygen flow of 50 sccm that gave a working pressure of 4.5×10^{-3} mbars.

To protect the Al from weathering damage, two different protective layers were compared, namely: 280 nm of sputtered SiO_2 and 4.5 μm of a commercial transparent hard coating. The thickness of the SiO_2 layer was optimized to give the highest reflectance and was grown under same conditions as the SiO_2 adhesive layer. The hard coat (CrystalCoatTM MP-101 from SDC Technologies) was a transparent hard-coat resin consisting of a siloxane matrix embedded with SiO_2 nanoparticles normally used to enhance the abrasion resistance of plastic. The hard-coat resin was dip-coated at a speed of 500 mm/min under a controlled constant humidity of 25%. The dip-coated mirror was then flashed off for 20 min and heated at 130°C for 45 min.

It is worth mentioning that the final mirror was compared to a commercial second surface solar mirror based on Ag and a 1 mm thick glass substrate.

2.2 Optical performance

The SR of the samples was assessed using a spectrophotometer Cary 5000 from Agilent. The spectra were recorded within the range 280 − 3300 nm at an angle of incidence of 7˚, and this was then used to calculate the solar-weighted specular reflectance ($\overline{SR}$) as per Eq. 1:

$$\overline{SR} = \frac{\int R \cdot I \cdot d\lambda}{\int I d\lambda} \times 100 \qquad (1)$$

Where R is the percentage reflectance at a given wavelength λ, I is the solar irradiance at that wavelength and dλ the wavelength interval of integration.

2.3 Morphology

The surface morphology of the Al films was analysed using an Atomic Force Microscope (AFM) Multimode 8 from Bruker in tapping mode. The Al films were imaged in tapping mode using tips from Budget Sensors (f_0 =300 kHz, k =40 Nm^{-1}) and NanoScope Analysis 1.5 was then used to calculate the root mean square roughness (Rq) values.

2.4 Adhesion, abrasion and hardness

The adhesion of the Al to the plastic substrate as well as the adhesion of the whole stack was determined using a standard cross-hatch tape adhesion test. A cross-hatch pattern was scored on the Al surface, and the Scotch tape was smoothly fixed over the pattern. After 60 s the tape was removed by hand in accordance with the industry testing procedure ASTM D3359-09e2 and the film subsequently observed under a microscope to examine the amount of material lost from the surface. Each measured sample was given a grading from 0B to 5B, where 0B represents ≥ 65% of the material removed, and 5B flawless adhesion (no material removed).

The abrasion resistance of the mirrors was determined by employing the Bayer and Steel Wool tests. In the Bayer test an Oscillating Abrasion Tester (model 6100) from Taber Industries was used to subject the samples to 300 cycles (150 cycles/min) immersed in 500 g of Al Zirconium Oxide (Alundum) as per variant of ASTM F753 standard. In the Steel Wool test a steel wool pad grade "0" with 50 μm fibre width was rubbed in a linear back and forth motion across the sample during 3 sets of 25 cycles (0.7 cycles/sec), with 1 minute pause between cycles, under an applied mass of 2 kg. For both tests the abrasion resistance was quantified by measuring the SR of the samples before and after abrasion. The smaller the difference between reflectance, the greater the abrasion resistance. SR was measured with a HunterLab UltraScan Pro instrument within the range 400-700 nm.

Nano-scratch tests were performed to evaluate the fracture resistance of the Al coatings deposited onto the differently treated substrates. The tests were performed using a UMIS2000 (CSIRO) with a spherical diamond tip (20 μm) creating a 2 mm scratch along the coating with a force that was linearly increased from 1 to 200 N.

2.5 Environmental durability

A salt-spray chamber from Ascott-Analytical Equipment was used to test the chemical resistance of the mirrors following test standard ASTM B117. A pass or fail criterion was determined by visual inspection and through assessing the change in the $\overline{SR}$ after a testing time of 40 days.

Accelerated weathering was performed with an Atlas Ci4000 weatherometer, with quartz inner and outer filters set to the SAE J1960 exposure standard. Post weathering tests were performed using SR measurements and visual assessment after the sample had been exposed to a total of 5 months, which is approximately equivalent to 5 years of natural weathering.

Real time natural outdoor weathering was also evaluated. Samples were placed onto a natural weather testing rack located at Mawson Lakes Campus, South Australia, Australia for a period of 5 months. Visual inspection and SR values were again used to evaluate the durability of the mirrors.

3. Results

3.1 Optimisation of the Al reflective layer

The Al thickness, the sputtering power density, the working pressure during deposition and the base pressure (before deposition) were varied in order to maximise the reflectivity of the Al film.

Figure 1 presents the $\overline{SR}$ of the Al films for thicknesses between 45 to 125 nm. All films were sputtered at a power density of 6.6 Wcm^{-2}, base pressure of 7.0×10^{-5} mbar and working pressure of 2.4×10^{-3} mbar. As observed in Figure 1 the $\overline{SR}$ experiences a rapid increase from 45 to 70 nm until reaching a maximum of 89.4% at 75-80 nm [25, 26], after which it plateaus to a slightly lower values. This small drop from 80 nm onwards is assigned to an increase of the film roughness [5, 27, 28]. Thus, based on this initial result a minimum thickness of 80 nm was chosen for all subsequent depositions.

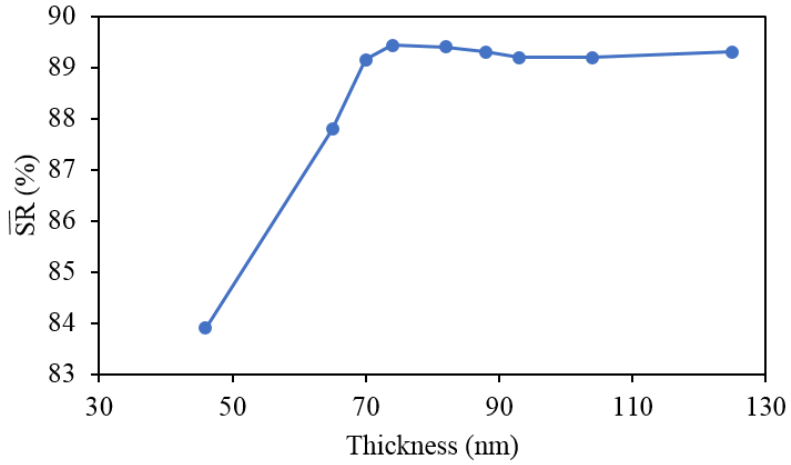


Figure 1. $\overline{SR}$ for 45−125 nm thick Al films deposited onto hard-coated PC substrates.

Having established the minimum film thickness the effect of sputtering power density and working pressure on the optical properties of Al were investigated next. Al films (80 nm) were deposited at power densities between 3.3 Wcm^{-2} and 13.2 Wcm^{-2}, at a base pressure of 7.0×10^{-5} mbar and under a working pressure of 2.4×10^{-3} mbar.

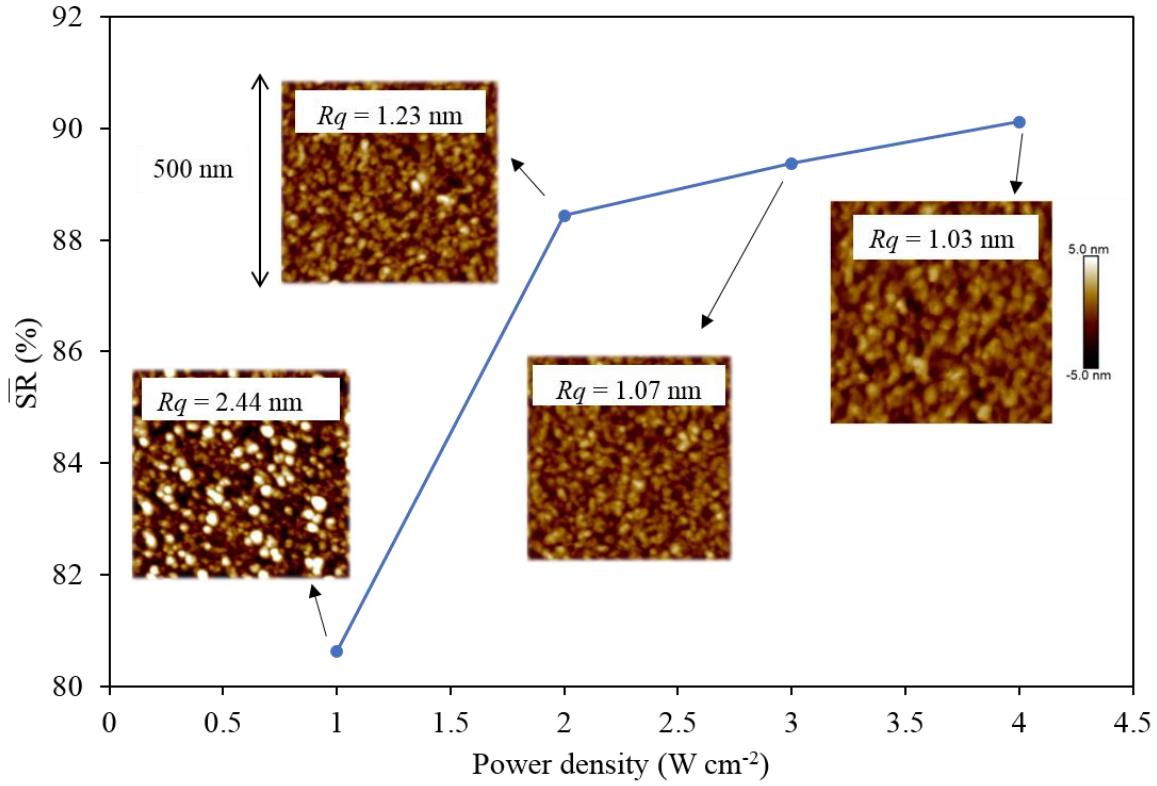


Figure 2. Effect of sputtering power density on the $\overline{SR}$ of 80 nm thick Al films deposited on hard-coated PC with their corresponding 500×500 nm AFM images and *Rq* values.

As shown in Figure 2 higher power densities resulted in an increase in the $\overline{SR}$ of the Al films with the largest improvement occurring between 3.3 and 6.6 Wcm^{-2}, but with gains continually recorded up to the maximum power density of 13.2 Wcm^{-2}. It is generally accepted that at high power, sputtered species reach the substrate with higher energy and tend to form densely packed films with small grains and low levels of surface roughness [29, 30]. To elucidate on this phenomenon and obtain an insight regarding the surface morphology, AFM images were taken of each sample, from which roughness values were extracted. As shown in the insets of Figure 2 the smoothest film (*Rq* = 1.03 nm) was the one grown at the highest power, which also recorded the highest specular reflective surface. Rough metallic surfaces have been reported as having lower SR values because of higher

reflected light scattering [31] and this was confirmed in the results presented herein. Worth noting is the fact that the largest improvement in $\overline{SR}$ coincided with the largest decrease in *Rq*, with modest improvements in $\overline{SR}$ for sputter power densities greater than 6.6 Wcm^{-2} correlating with marginal decreases in *Rq* values.

It was noted however, that with increasing power density, the adhesion of the Al to the hard-coated PC substrate was marginally reduced (refer Table 1: adhesion reduced from 5B down to 4B). One of the major influencing factors for Al adhesion to hard-coated polymeric substrates comes from the alumina passivation layer which is created at the substrate-Al interface during deposition [4, 5, 32]. At the higher power densities used in this study Al deposition may be occurring too rapidly, suggesting that the alumina interface layer was either too thin or poorly formed. The exact reason, however, is currently not well understood and is the subject of further study. Therefore 6.6 Wcm^{-2} rather than 13.2 Wcm^{-2} was employed as the power density for sputtering the Al layer, resulting in a small sacrifice in $\overline{SR}$ for a gain in film robustness (i.e. enhanced adhesion).

Table 1. Results of the adhesion tape test for sputtering power densities in the range 3.3-13.2 Wcm^{-2} for 80 nm thick Al films deposited on PC. A grade of 5B means complete adhesion (no loss of coating) while a grade of 0B implies that more than 65% of the material has been removed.

Power Density /Wcm^{-2}	3.3	6.6	9.9	13.2
Adhesion Grade	5B	5B	4B	4B

Al films (80 nm) were now deposited at working pressures between 1.0×10^{-3} mbar and 4.8×10^{-3} mbar, at a base pressure of 7.0×10^{-5} mbar and using a power density of 6.6 W cm^{-2}.

The working pressure at which sputtering processes take place have been shown to have a large influence on the energy at which the target atoms reach the substrate (see Figure 3) [29, 30]. The lower the pressure, the longer the mean free path of the target atoms and therefore, the higher the energy at which they reach the substrate. From 5×10^{-3} down to 3×10^{-3} mbar, the roughness decreased

and the resultant $\overline{SR}$ increased. However, at working pressures below 3×10^{-3} mbar the roughness increased once again which consequently decreased the $\overline{SR}$. Considering that the SR is related to the surface roughness (and the purity of the film) [5] it is likely that at such a low pressure, the deposition rate was low. Previous studies from Hora et al. [33] and Petrov et al. [34] have indicated that film formation (especially on polymeric substrates) is composed of a three-step process: nucleation, coalescence and growth. That this progression is governed by kinetic adsorption and the subsequent diffusion of the arriving species. Given the small change in *Rq* below the working pressure of 3×10^{-3} mbar, one can with justification assume that roughness alone is not responsible for the decrease in $\overline{SR}$. The slow film formation at such low working pressures does open up the possibility of secondary reactions taking place at the surface and thus one cannot discount the possibility of oxygen and other contaminants being incorporated into the film, hence, leading to reduced reflectance. Thus based on the results, an optimum working pressure of 2.4×10^{-3} mbar was selected (corresponding to a surface roughness of $\approx$ 1.04−1.08 nm) for Al film depositions.

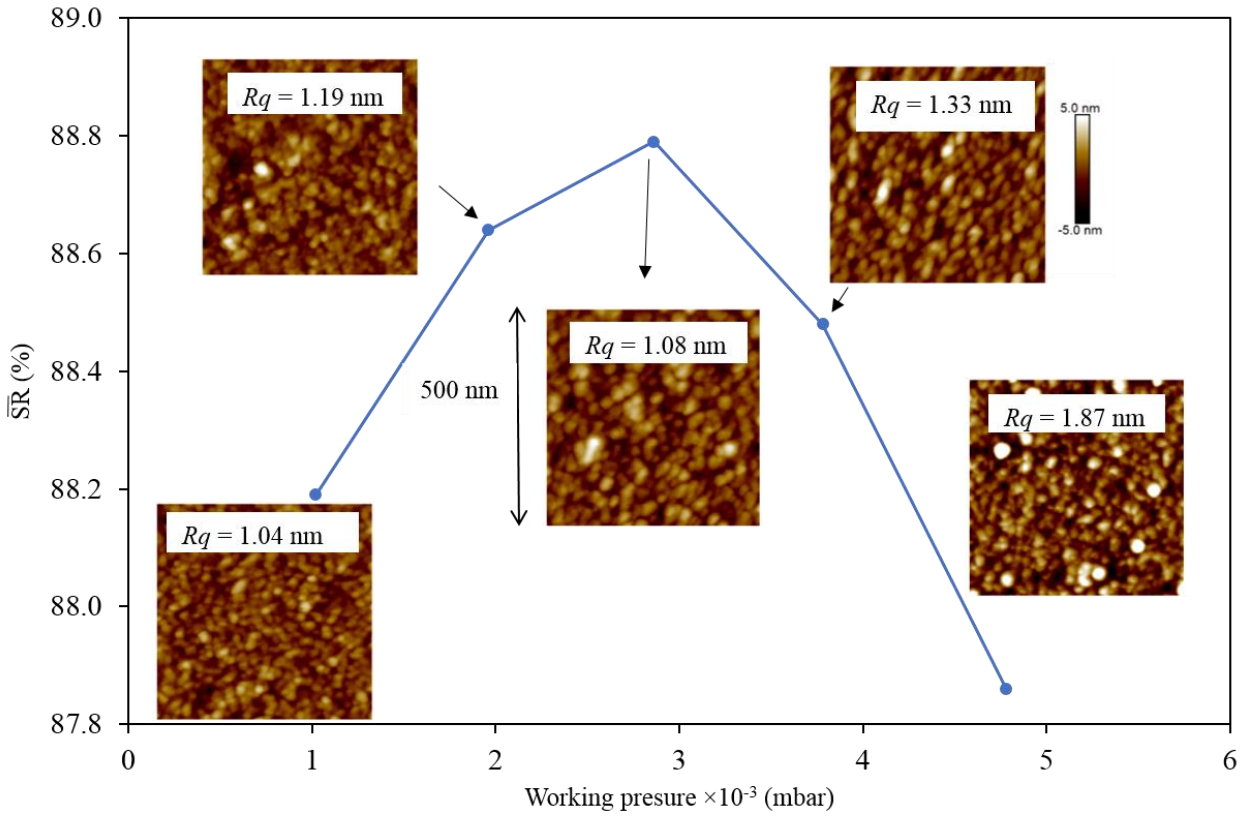


Figure 3. Effect of working pressure on the $\overline{SR}$ for 80 nm thick Al films deposited on PC with the corresponding 500×500 nm AFM images and *Rq* values.

In addition to the working pressure (during sputtering), the effect of base pressure (before deposition) on the reflectance of the Al samples was investigated. Al films (80 nm) were deposited at 6.6 W/cm^2, 2.4×10^{-3} mbar, at two different base pressure values, namely: the initially used 7×10^{-5} mbar and then followed by the lower value of 7×10^{-6} mbar. The film grown at a base pressure of 7×10^{-5} mbar upon initial visual inspection looked slightly "darker", with $\overline{SR}$ measurements confirming that at 7×10^{-6} mbar the value was as high as 91% in comparison to 89% for the same film deposited at the higher base pressure. The significant improvement in $\overline{SR}$ resulting from a lower base pressure of 7×10^{-6} mbar provided strong (albeit indirect) proof that fewer contaminants are being incorporated into the film during deposition. Having systematically established a process protocol (i.e. 80 nm film thickness, base pressure 7×10^{-6} mbar, working pressure 2.4×10^{-3} mbar and a power density of 6.6 Wcm^{-2}) for

the fabrication of high $\overline{SR}$ Al coated PC substrate mirrors exhibiting excellent adhesion, attention turned to optimising the protective overcoat layer.

3.2 Protective layer optimisation

Initially sputter deposited SiO_2 (280 nm) films were evaluated as the protective coating for the Al first surface mirrors on untreated PC substrates. The $\overline{SR}$ was reduced by ≈ 3% (see Figure 4) and the adhesion cross-hatch test resulted in a grade of 2B, exhibiting failure at the Al-substrate interface, an unacceptable value for commercial implementation of the mirror.

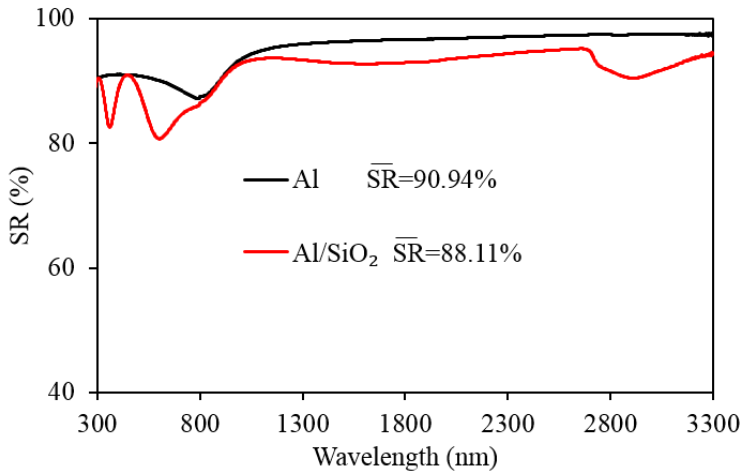


Figure 4. SR (λ) spectra of 80 nm of Al and 80 nm of Al with 280 nm of SiO_2 deposited on top.

This lack of adhesion is assigned to the greater chemical affinity of the Al atoms to the oxygen present in the SiO_2 rather than for the oxygen present at the surface of the substrate (i.e. there is a higher concentration of oxygen in the SiO_2 layer compared to the substrate). The Al therefore remained adhered to the SiO_2 and the PC-Al interface failed upon removal of the tape. As a consequence of the adhesion test failure three different substrate treatments were investigated in an attempt to improve the adhesion of the Al coating to the substrate. The PC was either: plasma cleaned using argon for 3 minutes, or, coated with a 15 nm SiO_2 seed layer or washed with isopropanol only (i.e. the control sample). The three differently treated substrate samples were then coated with 80 nm of Al and nano-scratch tests performed to ascertain the applied load at which film fracture first occurred [35, 36].

a)

Sample description	Critical Load /mN
Isopropanol cleaned PC/Al	110
Plasma cleaned PC/Al	128
PC /15 nm SiO_2/Al	133

b)

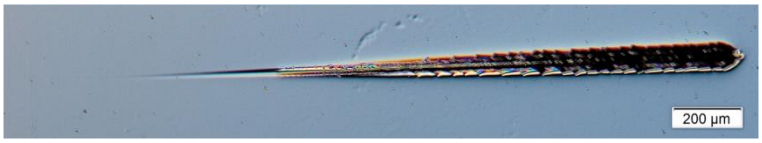


Figure 5. a) Nano-scratch critical load values required to initiate film fracture for the Al films deposited on three differently treated substrates b) Image of the nano-scratch track on an isopropanol cleaned PC substrate with an 80 nm Al deposition on top.

The nano-scratch test shown in Figure 5 indicated the fracture resistance of the Al films, with the critical load being the force applied to the tip, at which the film first fractures. After the initial fracture fluctuations in both force and penetration depth of the nano-scratch tip occurred, which marked the critical load point. The higher the critical load the better the adhesion of the film to the substrate [35]. From the results given in Figure 5 the highest critical load required to fracture the Al film was achieved when the SiO_2 seed layer was used to overcoat the PC substrate, followed by the plasma treatment and lastly by the isopropanol wash (i.e. control treatment). Worth noting was the fact that the plasma treated substrate also recorded a significant improvement in the critical load value in comparison to the isopropanol cleaned PC. This is due to increase in the surface energy of polymeric materials which can translate into better adhesion of the deposited films [37].

To confirm the nano-scratch results being related to film adhesion, 280 nm of SiO_2 was deposited onto the three differently treated PC substrates coated with 80 nm of Al and a suite of industry relevant tests applied, namely: adhesion, Bayer, Steel Wool and outdoor exposure tests were performed. The results are displayed in Table 2 where both the adhesion grade is recorded and the ΔSR is the difference in reflectivity before and after each test.

Table 2. Adhesion grade and change in reflectance (ΔSR) after Bayer and Steel Wool tests for the three different PC substrate treatments. Note: only the 15 nm SiO_2 treated PC sample was able to withstand 60 days outside weathering test, recording an additional drop in reflectance ($\Delta\,\overline{SR}$) of 2.8%. The other two samples degrading to the point of not being able to record any (usable) reflectance values.

Sample description	Adhesion grade	Bayer ΔSR (%)	Steel Wool ΔSR (%)	60 days outdoors $\Delta\,\overline{SR}$ (%)
Isopropanol cleaned PC/Al/SiO_2	2B	13.7	76.9	n/a
Plasma cleaned PC/Al/ SiO_2	3B	11.9	46.0	n/a
PC /15 nm SiO_2/Al/ SiO_2	5B	2.8	1.9	2.8

In agreement with the nano-scratch results, the Al deposited onto the plasma cleaned PC substrate showed an improvement in adhesion and abrasion resistance in comparison to that of the isopropanol cleaned PC substrate (i.e. 3B versus 2B adhesion grade). However, the Al coating deposited onto the 15 nm SiO_2 seed layer was the only sample able to withstand 60 days of natural weathering and a 5B adhesion result. Although most of the mirror's surface looked unchanged after the 60 day weathering trial, the small drop in reflectance revealed (i.e. $\Delta\,\overline{SR}$=2.8%) that some degradation, albeit small, had occurred. To further examine the sample, microscope images were taken at different points on the surface. Figure 6, shows a large dark region as well as the beginning of several (possible) pinholes (i.e. small dark spots), suggesting that the protective overcoat had been damaged to the point where the Al had been exposed to the atmospheric elements. Given the harsh abrasion tests conducted in this study such an outcome was not totally unexpected, with the small pinholes providing an ingress point for corrosion to occur. Such a phenomenon has been observed by others [38].

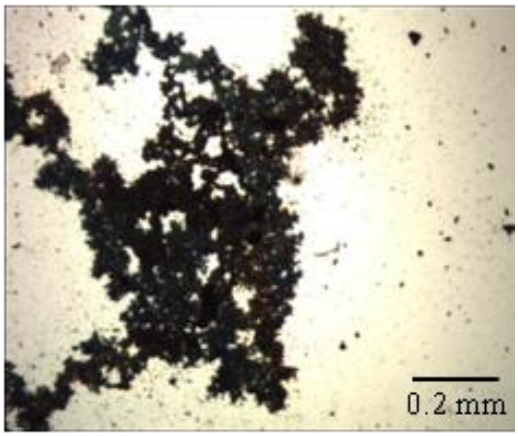


Figure 6. 1.2×1.0 mm microscope image of Al coated sample showing multiple pinholes (dark small spots) after exposure to 60 days of natural weathering. The large dark area indicates a region of corrosion where the pinhole has penetrated all the way down through the protective SiO_2 layer.

As an alternative to the SiO_2 protective layer, a commercial thermally cured hard-coat was used as a protective layer for the mirrors. The PC substrate was initially plasma cleaned for 3 minutes and then 15 nm of SiO_2 followed by 80 nm of Al were deposited using magnetron sputtering. The sample was then dip-coated with 4.5 µm of MP-101 (SDC Technologies) liquid hard coat resin followed by thermal curing step. The reflectivity before and after hard coating was measured and is presented in Figure 7.

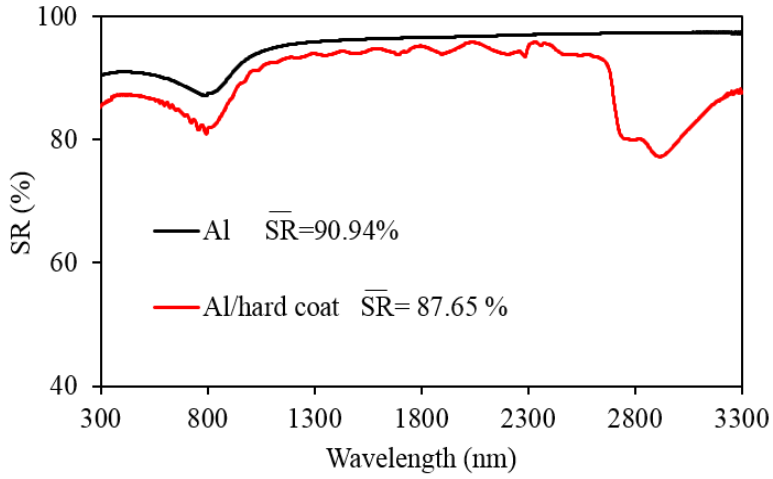


Figure 7. SR (λ) spectra for the 80 nm Al sample compared to the 80 nm Al sample with a 4.5 µm proprietary SiO_2 hard coat.

After coating the sample with 4.5 µm of MP-101, a perfect adhesion result was obtained (5B), and the reflectivity was only reduced by 3.3% which is similar to the decrease recorded with the addition of a 280 nm thick SiO_2 protective layer.

For comparison purposes a commercially available solar mirror was also tested. This was a second surface mirror which uses glass as the substrate, hence, the abrasion tests were performed on top of the glass. Abrasion and durability results of both our hard coated first surface mirror and the commercial mirror are presented in Table 3.

The reductions in reflectivity, for the Bayer and Steel Wool abrasion tests for the hard coat resin were 0.4% and 0.1% respectively, which is much smaller than the sample originally coated with the 280 nm sputtered SiO_2 layer and it is comparable or better (for the Bayer test) to that given by the commercial mirror.

Table 3. Results of the adhesion test, Bayer and Steel Wool tests, performed on the mirror sample over-coated with 4.5 µm of MP-101 and the commercially available second surface solar mirror. Change in solar-weighted specular reflectance ($\Delta\ \overline{SR}$) after an extended 5 months outdoor testing, 5 months under accelerated weather testing being equivalent to 5 years of natural weathering (as per SAE J1960 standard) and after 40 day under continuous salt-spray exposure.

Sample description	Bayer ΔSR (%)	Steel Wool ΔSR (%)	$\Delta\ \overline{SR}$ (%) 5 months natural weathering	$\Delta\ \overline{SR}$ (%) 40 days salt-spray	$\Delta\ \overline{SR}$ (%) after 5 months accelerated weathering
Plasma cleaned PC /15 nm SiO_2/Al/ hard coat	0.4	0.1	0.2	0.3	0.01

Commercial solar mirror	1.8	0	0	0	0

After 5 months of natural weathering no pinholes were noted in the coating and only a small change in the reflectance was observed (see Table 3, $\overline{SR}$=0.2%) suggesting that the hard coat resin was efficiently protecting the aluminium from corrosion. To further corroborate this outcome, and provide relevant evidence that the three-layer plastic mirror was durable enough to be commercially viable, salt spray tests and accelerated weathering were also performed. After 40 days in a salty-humid atmosphere (i.e. this is the harsh automotive industry standard for mirror products to be commercially acceptable and has been adopted as the minimum pass/fail protocol for the heliostat mirrors) the mirror upon visual inspection looked unchanged and its reflectance remained at ≈ 88%. Accelerated weathering was also executed for a period of 5 months which is the equivalent to 5 years of natural weathering. The mirror upon visual inspection looked unchanged and once again recorded a spectral reflectance of 88%. Thus initial results indicate that the three-layer mirror design discussed herein appears to meet the harsh (automotive industry adopted protocol) weathering requirements and is comparable to a commercially available second surface mirror. Further to the scope of this study, future work will systematically evaluate the thickness of the hard coating with respect to finding an optimised balance between high weathering protection and low impact on the SR.

4. Conclusions

An Al-based highly durable plastic mirror has been developed to be applied as part of a heliostat. The mirror has been optimized in order to produce a simple and low-cost configuration as well as to provide high durability and resistance to most extreme weather conditions. The architecture of the mirror consists of a three-layer stack deposited onto a commercially available Makrolon AR PC, cleaned with an Ar plasma prior to use. The first layer is a 15 nm sputtered SiO_2 coating which acts

as the adhesive layer between the Al and the substrate. The second layer is the Al film of which the reflectance has been optimized by varying the: thickness, sputtering power density, working pressure and base pressure. Optimum conditions (base pressure of 7×10^{-6} mbar, working pressure of 2.40×10^{-3} mbar and power density of 6.6 Wcm^{-2}) gave a $\overline{SR}$ of ≈ 91% in the wavelength range 280-3300 nm for an 80 nm thick Al film. For the third and final layer, the mirrors were coated with a commercial transparent hard coat resin (MP-101) that was 4.5 μm thick, which reduced the total reflectivity to 88% but produced outstanding abrasion resistance and durability. This was demonstrated by: adhesion tests, Bayer, Steel Wool, salt-spray (40 days) and both outdoor and accelerated weathering tests for a duration of 5 months.

Acknowledgements

We gratefully acknowledge research funding support from the Automotive Australia 2020 CRC and Precision Components Pty Ltd.

This work was performed in part at the South Australian node of the Australian National Fabrication Facility under the National Collaborative Research Infrastructure Strategy.

Author information

Corresponding Author:
Email: marta.lluscajane@unisa.edu.au
ph: +61 8 830 25174

ORCID:
Marta Lluscà Jane: 0000-0002-4260-6305
Manrico Fabretto: 0000-0002-8121-198X
Kamil Zuber: 0000-0003-0579-1983
Eric Charrault: 0000-0003-3392-136X
Peter Murphy: 0000-0002-5127-8120
Apurva Patil: 0000-0003-2145-1081

References

[1] Ennaceri, H.; Benyoussef, A.; Ennaoui, A.; Khaldoun, A. Optical properties of front and second surface silver-based and molybdenum-based mirrors. *Int. J. Res. Eng. Technol*. **2016**, *8*, 410–413.

[2] Advanced Reflector and Absorber Materials (Fact Sheet), report, August 1, 2010; Golden, Colorado. (https://digital.library.unt.edu/ark:/67531/metadc1012196/: accessed May 6, 2019), University of North Texas Libraries, Digital Library, https://digital.library.unt.edu; crediting UNT Libraries Government Documents Department.

[3] Hass, G. Reflectance and preparation of front-surface mirrors for use at various angles of incidence from the ultraviolet to the far infrared. *J. Opt. Soc. Am*. **1982**, *72*, 27.

[4] Benjamin, P.; Weaver, C. The Adhesion of Evaporated Metal Films on Glass. *Proc. R. Soc. Lond. A.* **1961,** *261*, 516–531.

[5] James, R. A.; Stapleton, A. J.; Hughes, A.; Charrault, E.; Zuber, K.; Switalska, E.; Evans, D.; Murphy, P.; Llusca, M. Metallic Adhesive Layers for Ag-Based First Surface Mirrors. *Adv. Eng. Mater*. **2018**, *20*, 1800106.

[6] Franey, J. P.; Kammelott, G. W.; Graedel, T. E. The corrosion of silver by atmospheric sulfurous gases. *Corr. Sci.* **1985**, *25*, 133−143.

[7] Graedel, T. E. Corrosion mechanisms for silver exposed to the atmosphere, *J. Electrochem. Soc*. **1992**, *139*, 1963–1969.

[8] Bennett, H. E.; Peck, R. L.; Burge, D. K.; Bennett, J. M. Formation and Growth of Tarnish on Evaporated Silver Films, *J. Appl. Phys*, **1969**, *40*, 3351–3360.

[9] E.D Palik (Ed.), Handbook of Optical Constants of Solids, Academic Press, Boston (1991)

[10] Heller, P.; Haberle, A.; Malbranche, P.: Mal, O.; Cabeza, L. F. Strategic energy technology plan-scientific assessment in support of the materials roadmap enabling low carbon energy technologies: concentrating solar power technology. *JRC Scientific and Technical Reports* **2011**, *67840.*

[11] Kennedy, C.; Smilgys, R.V.; Kirkpatrick, D. A.; Ross, J. S. Optical performance and durability of solar reflectors protected by an alumina coating. *Thin Solid Films* **1997**, *304,* 303-309.

[12] Morales, A.; Ajona, J. Durability, performance and scalability of sol–gel front surface mirrors and selective absorbers. *J. Phys. IV* **1999,** *9,* 513–518.

[13] Morales, A.; Ajona, J. Durability and performance test of sol–gel front surface silver mirrors. *Proc. 8th Int. Symposium on Solar Thermal Concentrating Technologies* **1996**, pp 463–476.

[14] Almanza, R.; Hernandez, P.; Martinez, I.; Mazari, M. Development and mean life of aluminum first-surface mirrors for solar energy applications, *Sol. Energy Mater. Sol. Cells* **2009**, *93*, 1647–1651.

[15] Xu, Y. J.; Cai, Q. W.; Yang, X. X. Zuo, Y. Z. Song, H.; Liu, Z. M.; Hang, Y. P. Preparation of novel SiO_2 protected Ag thin films with high; reflectivity by magnetron sputtering for solar front reflectors, *Sol. Energy Mater Sol. Cells* **2012**, *107,* 316–321.

[16] Xu, Y. J.; Liao, J. X.; Cai, Q.W.; Yang, X. X.; Preparation of a highly-reflective TiO_2/SiO_2/Ag thin film with self-cleaning properties by magnetron sputtering for solar front reflectors, *Sol. Energy Mater Sol. Cells* **2013**, *113*, 7–12.

[17] Ennaceri, H.; Erfurt, D.; Wang, L.; Köhler, T.; Taleb, A.; Khaldoun, A.; Kenz, A.E.; Benyoussef, A.; Ennaoui, A. Deposition of multifunctional TiO_2 and ZnO top-protective coatings for CSP application, *Surf. Coat. Tech.* **2016**, *298,* 103–113.

[18] Schissel, P.; Jorgensen, G.; Kennedy, C.; Goggin, R. Silvered-PMMA reflectors. *Sol. Energy Mater Sol. Cells* **1994,** *33,* 183−197.

[19] Price H,; Lüpfert E.; Kearney D.; Zarza E.; Cohen G.; Gee R. Advances in parabolic trough solar power technology. *J. Sol. Energy Eng. Trans.* ASME **2002**, *124*, 109–25.

[20] Kennedy C. E.; Smilgys R.V.; Kirkpatrick D. A.; Ross J. S. Optical performance and durability of solar reflectors protected by an alumina coating technical report No. NREL/TP-471-21413. Golden: NREL; **1996**.

[21] Karim, M.; Naamane, S.; Hassani, I. E. A. E.; Delord, C.; Belcadi, S.; Tochon, P.; Bennouna A. Towards the prediction of CSP mirrors wear: Methodology of analysis of influencing parameters on the mirrors surface degradation: Application in two different sites in Morocco, *Sol. Energy*, **2014**, *108*, 41−50.

[22] Dennis W. E.; McGee J. B. Silicone resins for protection of first surface reflectors. *Sol. Energy Mater.* **1980,** *3*, 285−300.

[23] Höflich, A.; Bradley, N.; Hall, C.; Evans, D.; Murphy, P.; Charrault, E. Packing density/surface morphology relationship in thin sputtered chromium films, *Surf. Coat. Technol*., **2016**, *291*, 286–291.

[24] Musil, J.; Vlcek, J.; Baroch, P.; Pauleau, Y. Magnetron discharges for thin films plasma processing. *Mater. Surf. Process. Directed Energy Tech.* **2006**, *1*, 67−110.

[25] Hass, G.; Waylonis, J. E. Optical constants and reflectance and transmittance of evaporated aluminum in the visible and ultraviolet. *J. Opt. Soc. Am.* **1961**, *51*, 719-722.

[26] Ehrenreich, H.; Philipp, H. R.; Segall, B. Optical properties of aluminum. *Phys. Rev.* **1963**, *132*, 1918.

[27] Quintana, P.; Oliva, A. I.; Ceh, O.; Corona, J. E.; Aguilar, M. Thickness effects on aluminum thin films. *Superficies y vacío* **1999**, *9*, 280−282.

[28] Xu, Y. J.; Cai, Q. W.; Yang, X. X.; Zuo, Y. Z.; Song, H.; Liu, Z. M.; Hang, Y. P. (2012). Preparation of novel SiO_2 protected Ag thin films with high reflectivity by magnetron sputtering for solar front reflectors. *Sol. Energy Mater Sol. Cells* **2012**, *107*, 316−321.

[29] Jung, Y. S. Study on texture evolution and properties of silver thin films prepared by sputtering deposition, *Appl. Surf. Sci*. **2004**, *221*, 281−287.

[30] M. Ohring, The Materials Science of Thin Films, Academic Press, 1992.

[31] Evans, D.; Zuber, K.; Hall, C.; Griesser, H. J.; Murphy, P. Abrasion resistance of thin film coatings as measured by diffuse optical scattering. *Surf. Coat. Tech.* **2011**, *206*, 312−317.

[32] Chapman, B. N. Thin-film adhesion. *J. Vac. Sci. Technol*. **1974**, *11*, 106−113.

[33] Hora, J.; Hall, C.; Evans, D.; Charrault, E. Inorganic Thin Film Deposition and Application on Organic Polymer Substrates. *Adv. Eng. Mater*, **2018**, *20*, 1700868.

[34] Petrov, I.; Barna, P. B.; Hultman, L.; Greene, J. E. Microstructural evolution during film growth. *J. Vac. Sci. Technol A* **2003**, *21*, S117−S128.

[35] Markanday, J. F.; Charrault, E.; Evans, D., Zuber, K.; Hall, C. Chemical seeding via propanol plasma pretreatment for improving adhesion and properties of PECVD siloxane coatings on polymers. *Plasma Process Polym*. **2017**, *14*, 1600106.

[36] Bull, S. J.; Berasetegui, E. G. An overview of the potential of quantitative coating adhesion measurement by scratch testing. *Tribol. Int.* **2006**, *39*, 99−114.

[37] Belkind, A.; Gershman. S. Plasma cleaning of surfaces. *Vac. Coat. and Tech*. **2008,** 46−57.

[38] Sutter, F.; Heller, P.; Fernandez-García, A.; Kennedy, C.; López-Martín, R.; Meyen, S.; Pitz-Paal, R. Methods for service life time estimation of aluminum reflectors. *Proceedings of SolarPACES* **2011**.